PLOS ONE

RESEARCH ARTICLE

Ethanol and High Cholesterol Diet Causes Severe Steatohepatitis and Early Liver Fibrosis in Mice

Yasodha Krishnasamy[1], Venkat K. Ramshesh[1], Monika Gooz[1], Rick G. Schnellmann[1,2], John J. Lemasters[1,3,4], Zhi Zhong[1]*

1 Department of Drug Discovery & Biomedical Sciences, Medical University of South Carolina, Charleston, South Carolina, United States of America, **2** Ralph H. Johnson Veterans Affairs Medical Center, Charleston, South Carolina, United States of America, **3** Department of Biochemistry & Molecular Biology, Medical University of South Carolina, Charleston, South Carolina, United States of America, **4** Institute of Theoretical & Experimental Biophysics, Russian Academy of Sciences, Pushchino, Moscow Region, Russian Federation

* Zhong@musc.edu

Citation: Krishnasamy Y, Ramshesh VK, Gooz M, Schnellmann RG, Lemasters JJ, Zhong Z (2016) Ethanol and High Cholesterol Diet Causes Severe Steatohepatitis and Early Liver Fibrosis in Mice. PLoS ONE 11(9): e0163342. doi:10.1371/journal.pone.0163342

Editor: Kwan Man, The University of Hong Kong, HONG KONG

Received: July 5, 2016

Accepted: September 7, 2016

Published: September 27, 2016

Data Availability Statement: All relevant data are within the paper.

Funding: This work was supported, in part, by Grants AA017756, DK073336 and DK037034 from the National Institutes of Health. The Cell & Molecular Imaging Core of the Hollings Cancer Center at the Medical University of South Carolina supported by NIH Grant 1P30 CA138313 and the Shared Instrumentation Grant S10 OD018113 provided instrumentation and assistance for SHG microscopy. Animals were housed in the Animal Resources at Medical University of South Carolina

Abstract

Background and Aim

Because ethanol consumption is commonly associated with a high cholesterol diet, we examined whether combined consumption of ethanol and high cholesterol increases liver injury and fibrosis.

Methods

Male C57BL/6J mice were fed diets containing: 1) 35% of calories from corn oil (CTR), 2) CTR plus 0.5% (w/v) cholesterol (Chol), 3) CTR plus ethanol (27% of calories) (EtOH), or 4) EtOH+Chol for 3 months.

Results

In mice fed Chol or EtOH alone, ALT increased to ~160 U/L, moderate hepatic steatosis occurred, and leukocyte infiltration, necrosis, and apoptosis increased modestly, but no observable fibrosis developed. By contrast in mice fed EtOH+Chol, ALT increased to ~270 U/L, steatosis was more extensive and mostly macrovesicular, and expression of proinflammatory molecules (HMGB-1, TLR4, TNFα, ICAM-1) and leukocyte infiltration increased substantially. Necrosis and apoptosis also increased. Trichrome staining and second harmonic generation microscopy revealed hepatic fibrosis. Fibrosis was mostly sinusoidal and/or perivenular, but in some mice bridging fibrosis occurred. Expression of smooth muscle α-actin and TGF-β1 increased slightly by Chol, moderately by EtOH, and markedly by EtOH+Chol. TGF-β pseudoreceptor BAMBI increased slightly by Chol, remained unchanged by EtOH and decreased by EtOH+Chol. MicroRNA-33a, which enhances TGF-β fibrotic effects, and phospho-Smad2/3, the down-stream signal of TGF-β, also increased

supported by NIH Grant C06 RR015455. The funders had no role in study design, data collection and analysis, decision to publish, or preparation of the manuscript.

Competing Interests: The authors have declared that no competing interests exist.

more greatly by EtOH+Chol than Chol or EtOH. Metalloproteinase-2 and -9 were decreased only by EtOH+Chol.

Conclusion

High dietary cholesterol and chronic ethanol consumption synergistically increase liver injury, inflammation, and profibrotic responses and suppress antifibrotic responses, leading to severe steatohepatitis and early fibrosis in mice.

Introduction

Alcoholic liver disease (ALD) affects more than 2.5 million people in U.S [1,2]. The pathological changes of human ALD are characterized in three major categories: steatosis, hepatitis, and fibrosis/cirrhosis, the last of which ultimately leads to end-stage liver disease and frequently liver cancer [1,2]. These three pathological types can exist independently but often co-exist. ALD accounts for ~50% of deaths due to cirrhosis and ~30% of all liver disease-related deaths in the U.S [3–7]. Death is also a frequent outcome when inflammation of the liver occurs [8,9]. Cirrhosis superimposed with alcoholic hepatitis results in a death rate of more than 60% over 4-years [10]. Despite extensive studies, mechanisms by which ethanol damages the liver are far from clear, and effective treatment for ALD is lacking. For patients with cirrhosis and liver failure, nutrition and supportive care are the major therapies. However, these treatments at best only delay progression of ALD.

ALD is frequently the result of heavy drinking. However, other co-existing risk factors markedly increase liver injury and fibrosis [2,10]. Gender, chronic viral hepatitis, HIV infection, hemochromatosis, genetic factors, obesity, and smoking all affect the progression of ALD. Nutritional factors also appear to play an important role in ethanol-induced liver injury and fibrosis/cirrhosis [10,11], and alcohol in combination with malnutrition increases ALD in human and in animals [12,13]. Fish oil and corn oil promote whereas beef fat decreases ethanol-induced liver injury [11,14].

Epidemiological studies show that high cholesterol intake is associated with increased risk of liver fibrosis and cancer [15]. Some recent reports indicate that high cholesterol intake exacerbates liver fibrosis after bile duct ligation, carbon tetrachloride treatment, methionine-choline deficiency (3 months) and high fat diet (6 months) in mice [16,17]. Since ethanol consumption and high cholesterol intake frequently co-exist in Western diets, we examined the combined effects of chronic ethanol and high cholesterol intake on liver injury and fibrosis.

Methods

Animals

Male C57BL/6J mice (8–10 weeks) from Jackson Laboratory were fed one of four modified Lieber-DeCarli liquid diets (Dyets, Bethleham, PA): 1) a control liquid (CTR) diet with 35% calories from corn oil and 27% of calories from maltose dextrin (Dyets), 2) a high cholesterol diet (Chol) with 0.5% (W/V) cholesterol (Dyets) added to CTR, 3) an ethanol (EtOH) diet with 35% calories from corn oil and 27% of calories from ethanol, and 4) an ethanol plus cholesterol (EtOH+Chol) diet with 35% calories from corn oil, 27% of calories from ethanol and 0.5% (W/V) cholesterol. Concentrations of ethanol in liquid diets were increased stepwise (9% of calories every 2 days), and mice were then fed the liquid diets for 3 months after

ethanol reached 27% of calories. In preliminary studies, we found that Chol did not alter the volume of diet consumption, whereas EtOH decreased diet consumption. Therefore, daily consumption of ethanol-containing liquid diets (EtOH and EtOH+Chol) were measured, and the same volumes were given to the CTR and Chol groups on the following day (pair-feeding) to balance caloric intake.

Measurement of serum alanine aminotransferase (ALT)

After 3 months of liquid diet feeding, the abdomen was opened under pentobarbital anesthesia (80 mg/kg, *i.p.*), and blood was collected from inferior vena cava. Serum was obtained by centrifugation and kept at -80°C. Alanine transaminase (ALT) was measured using a kit from Pointe Scientific (Canton, MI).

Measurement of hepatic triglycerides, total cholesterol, and hydroxyproline

Hepatic triglycerides in liver homogenates were extracted with 2:1 chloroform/methanol and measured using an analytical kit (Enzymatic Standbio, Boerne, TX), as described previously [18]. After hydrolyzing liver tissue in sodium hydroxide (2N) at 120°C, hydroxyproline was detected as described elsewhere and expressed as μg/g liver wet weight [19].

To measure cholesterol, liver tissue (10 mg) was homogenized in 200 μL of a mixture of chloroform:isopropanol:NP-40 (7:11:0.1) and then centrifuged at 15,000X g for 10 min at room temperature. The supernatant (organic phase) was transferred to a new tube, dried in air at 50°C on a hotplate until the solvents were removed, and then kept under vacuum at room temperature for 30 min to remove trace amounts of solvents. The resulting lipid pellets were dissolved in 200 μl of 1x assay diluent from the Total Cholesterol Assay Kit (Cell Biolabs Inc, San Diego, CA). Cholesterol in 50 μl of samples was measured using the assay kit according to the manufacturer's protocol.

Histology and detection of fibrosis on liver sections

Under pentobarbital anesthesia as described above, the liver was infused with ~2 mL normal saline and then harvested. Liver tissue was fixed in 4% paraformaldehyde in phosphate buffer for 48 h and processed for paraffin sections [20]. Liver sections were stained with hematoxylin and eosin (H&E), and images were captured under a microscope (Zeiss Axiovert 100 microscope, Thornwood, NY) using a 20x objective lens.

Some liver slides were processed at the Histological Core of Medical University of South Carolina and stained with the Mason's Trichrome staining to reveal liver fibrosis. Images were captured using a Zeiss Axiovert 100 microscope (Thornwood, NY) and a 10x objective lens [20].

Additionally, liver fibrosis was detected by second harmonic generation (SHG) microscopy of liver sections. When intense laser light passes through a material with a non-linear molecular structure such as collagen, the interaction of laser light with the nonlinear material generates second-harmonic light which possesses twice the energy but half the wavelength of the original light [21]. Therefore, collagen fibers can be imaged by SHG without special staining or fluorophores. On de-paraffinized, unstained slides, SHG imaging was performed using an Olympus FluoView 1200MPE laser scanning multiphoton microscope (Olympus, Center Valley, PA) and a 30x 1.2 N.A. water-immersion objective lens. Second harmonic imaging was performed with 900-nm light. The emission wavelength was 450 nm [22].

Immunoblotting

After liver harvest under pentobarbital anesthesia, liver tissue was snap-frozen in liquid nitrogen and kept at -80°C until use. Proteins of interest were detected by immunoblotting, as described previously [20]. Membranes were blotted with primary antibodies against cleaved caspase-3 (CC3), fatty acid synthase (FAS), actin (Cell Signaling Technology, Danvers, MA), myeloperoxidase (MPO, DAKO Corp., Carpinteria, CA), CD4 (Origene Technologies, Rockville, MD), high mobility group box-1 (HMGB-1), toll-like receptor-4 (TLR4), Type I collagen, transforming growth factor-β1 (TGF-β1), cytochrome p450 2E1 (Cyp2E1) (Abcam, Cambridge, MA), 4-hydroxynonenal adducts (4-HNE, Alpha Diagnostic, San Antonio, TX), Smad2/3 and phospho-Smad2/3, bone morphogenic protein and activin membrane-bound inhibitor (BAMBI), alcohol dehydrogenase (ADH), aldehyde dehydrogenase-2 (ALDH2), carnitine palmitoyltranferase-1 (Cpt1) (Santa Cruz Biotech., Santa Cruz, CA), metalloproteinase-2 (MMP-2, Calbiochem, Billerica, MA), metalloproteinase-9 (MMP-9), intracellular adhesion molecule-1 (ICAM-1; BD Biosciences Pharmingen, San Diego, CA), F4/80 (Serotech, Raleigh, NC), and smooth muscle α-actin (α-SMA, DAKO, Carpinteria, CA) at concentrations of 1:1000 to 1:3000 overnight at 4°C. Horseradish peroxidase-conjugated secondary antibodies of appropriate species were then applied, and detection was by chemiluminescence (Pierce Biotechnology, Rockford, IL).

Detection of the X-box binding protein 1 (XBP-1) mRNA by quantitative real-time PCR

The mRNA of XBP-1 was detected by RT-qPCR, as described elsewhere [20], using the following primers: forward: `ACACGCTTGGGAATGGACAC` and reverse: `CCATGGGAAGATGTT CTGGG`. The abundance of mRNAs was normalized against hypoxanthine phospho-ribosyltransferase (HPRT) using the $\Delta\Delta Ct$ method.

Detection of miRNA 33a in liver tissue

Small RNA (<100 nucleotides) enriched in miRNA was extracted from liver tissue using High Pure™ miRNA isolation kit (Roche®, Indianapolis, IN) according to the manufacturer's protocol. cDNAs were synthesized from 10 ng RNA using Universal cDNA synthesis Kit (Exiqon, Woburn, MA). Real-time PCR reaction was performed using a miRCURY™LNA Real-time PCR kit (Exiqon) and the Bio-rad CFX 96 Real time PCR System with incubation at 95°C for 10 min, followed by 40 cycles at 95°C for 15 seconds and 60°C for 1 min. The sequence of miRNA-33a probe is 5'-`GUGCAUUGUAGUUGCAUUGCA`-3'. The results were normalized to the expression of U6 miRNA (the reference gene, probe sequence: 5'-`GTGCTCGCTTCGGCAGCA CATATACTAAAATTGGAACGATACAGAGAAGATTAGCATGGCCCCTGCGCAAGGATGACACG CAAATTCGTGAAGCGTTCCATATTTT`-3'). Differential expression was determined by the delta-delta Ct method.

Statistical analysis

Data shown are means ± S.E.M. (4 mice per group). Groups were compared using ANOVA plus Student-Newman-Keuls posthoc test. Differences were considered significant at $p<0.05$.

Ethics statement

All animals were given humane care in compliance with institutional guidelines using protocols approved by the Institutional Animal Care and Use Committee of the Medical University of South Carolina. All surgery was performed under sodium pentobarbital anesthesia (80 mg/kg, *i.p.*).

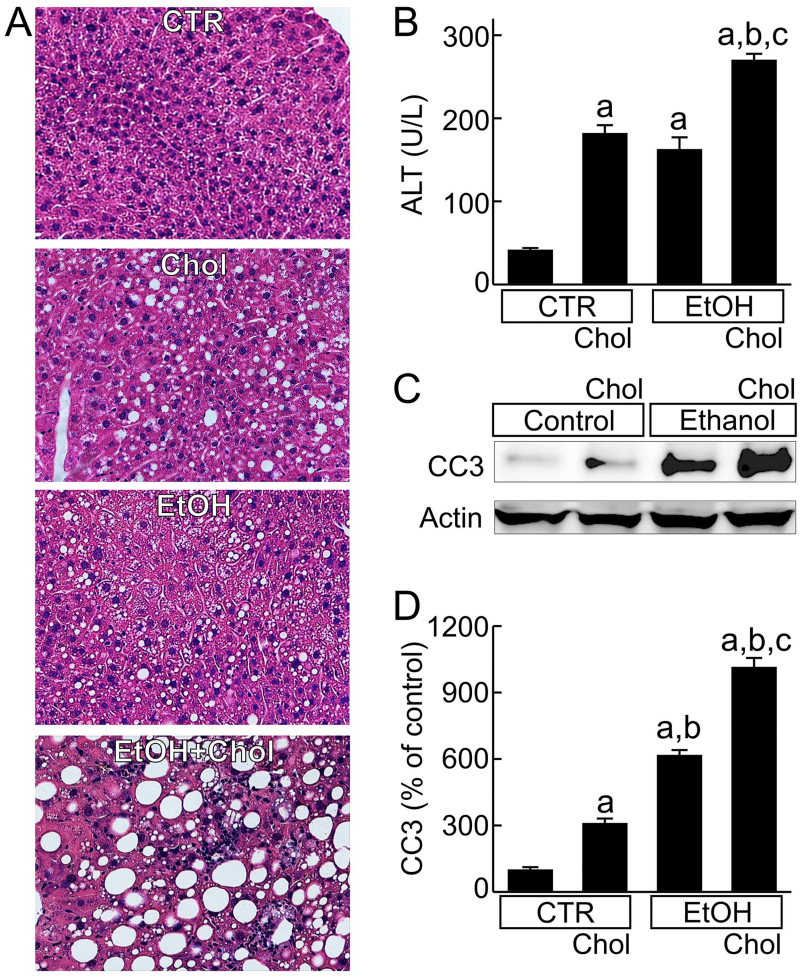

Fig 1. Combined ethanol and cholesterol feeding exacerbates liver injury and steatosis. Mice were fed CTR, Chol, EtOH or EtOH+Chol diets for 3 months. **A**, representative images from H&E stained liver sections. **B**, serum alanine aminotransferase (ALT). **C**, representative immunoblots of cleaved caspase-3 (CC3) and actin. **D**, quantification of CC3 immunoblots by densitometry. Values are means ± S.E.M. **a**, $p < 0.05$ vs CTR; **b**, $p < 0.05$ vs Chol; **c**, $p < 0.05$ vs EtOH ($n = 4$ per group).

doi:10.1371/journal.pone.0163342.g001

Results

Combined chronic ethanol consumption and high cholesterol intake increase liver steatosis and injury

In the livers from mice fed CTR, no pathological changes were observed, only some small fat droplets (Fig 1A). After feeding either Chol or EtOH, steatosis developed with mixed micro- and macrovesicular fat droplets. Steatosis was slightly greater in the Chol group than the EtOH group (Fig 1A). By contrast after EtOH+Chol feeding, much more marked steatosis developed with widespread formation of macrovesicular fat droplets that were larger in size and more abundant compared to Chol or EtOH (Fig 1A).

Hepatic triglycerides increased 8-fold and 6-fold, respectively, after feeding Chol and EtOH diets (Fig 2A). By contrast after EtOH+Chol, triglycerides increased 13-fold (Fig 2A). Hepatic cholesterol increased 2.3-fold and 1.7-fold, respectively, with the Chol and EtOH diets (Fig 2B), whereas after feeding EtOH+Chol, hepatic cholesterol increased 3.7-fold (Fig 2B).

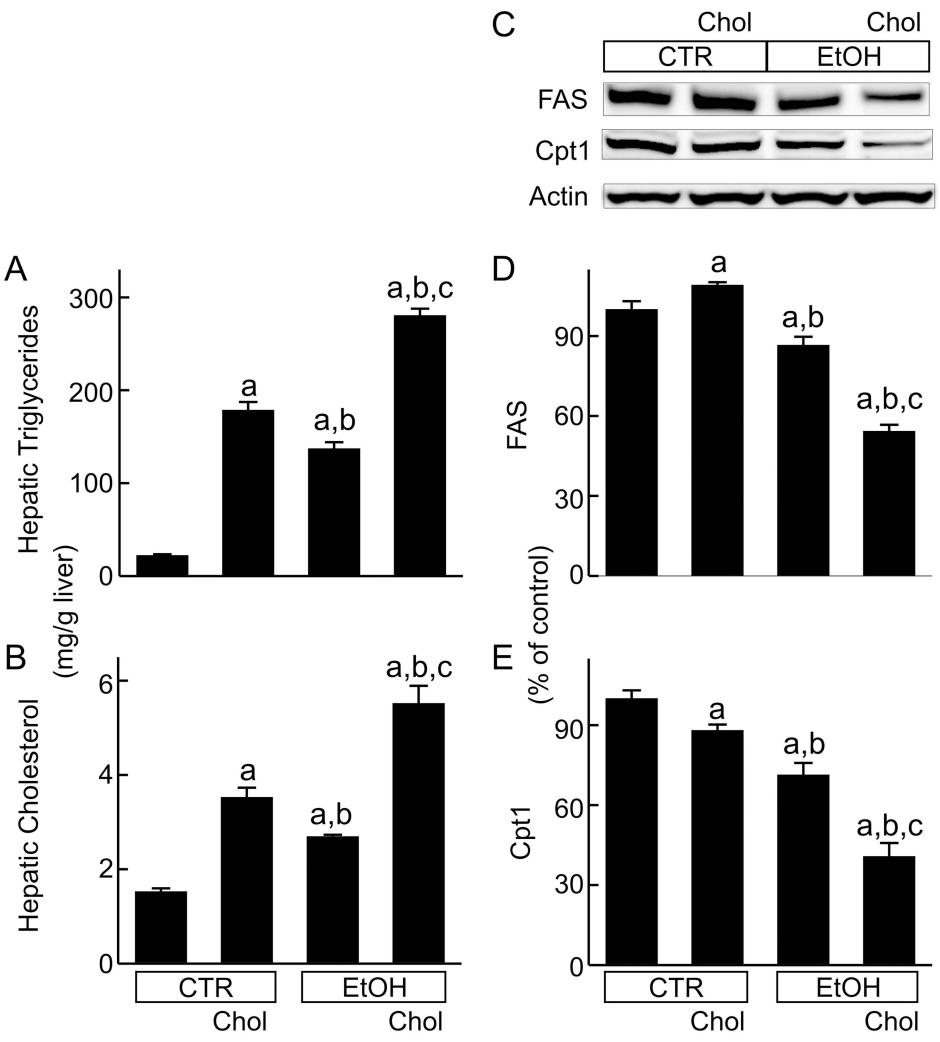

Fig 2. Combined ethanol and cholesterol feeding increases hepatic triglycerides and cholesterol but suppressed fatty acid synthase and carnitine palmitoyltransferase-1 expression. Mice were fed CTR, Chol, EtOH and EtOH+Chol diets for 3 months. Triglycerides (**A**) and cholesterol (**B**) in liver extracts were measured using commercial kits. FAS and Cpt1 were detected by immunoblotting (**C**, representative images). **D**, quantification of FAS immunoblots by densitometry. **E**, quantification of Cpt1 immunoblots. Values are means ± S.E.M. **a**, $p < 0.05$ vs CTR; **b**, $p < 0.05$ vs Chol; **c**, $p < 0.05$ vs EtOH (n = 3–4 per group).

doi:10.1371/journal.pone.0163342.g002

FAS, which catalyzes *de novo* fatty acid formation, increased slightly (9%) by Chol but decreased 13% by EtOH and 46% by EtOH+Chol (Fig 2C and 2D). Cpt1 catalyzes the transfer of the fatty acyl groups from coenzyme A (CoA) to carnitine to form palmitoylcarnitine, an essential step for transport of long chain fatty acids into mitochondria for β-oxidation [23]. After Chol and EtOH, respectively, Cpt1 decreased 12% and 29%, whereas after EtOH+Chol Cpt1 decreased 59% (Fig 2E).

Compared to CTR, serum ALT levels increased 4-fold after feeding Chol or EtOH. By contrast after feeding EtOH+Chol, serum ALT increased 6.4-fold (Fig 1B), indicating greater liver injury. Necrosis, apoptosis, and ballooning degeneration were observed in the livers from Chol-fed or EtOH-fed mice. These changes became more overt in livers from EtOH+Chol-fed mice (Fig 1A). Cleaved caspase-3, a marker of apoptosis, increased 3.1-fold by Chol, 6.1-fold by EtOH, and 10.1-fold by EtOH+Chol (Fig 1C and 1D).

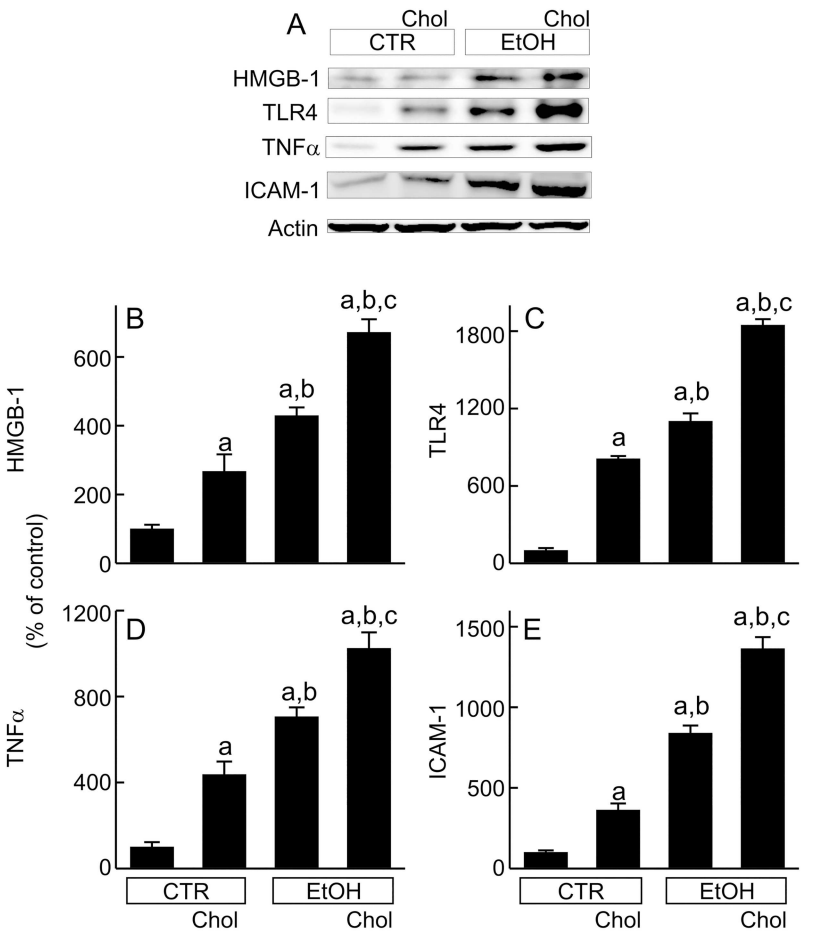

Fig 3. Combined ethanol and cholesterol feeding enhances inflammatory responses. Mice were fed CTR, Chol, EtOH and EtOH+Chol diets for 3 months. **A**, representative immunoblots of HMGB-1, TLR4, TNFα, ICAM-1 and actin. **B**, quantification of HMGB-1 immunoblots by densitometry. **C**, quantification of TLR4 immunoblots. **D**, quantification of TNFα immunoblots. **E**, quantification of ICAM-1 immunoblots. Values are means ± S.E.M. **a**, $p < 0.05$ vs CTR; **b**, $p < 0.05$ vs Chol; **c**, $p < 0.05$ vs EtOH ($n = 4$ per group).

doi:10.1371/journal.pone.0163342.g003

Combined chronic ethanol and high cholesterol intake synergistically increases inflammatory responses in the liver

HMGB-1 is up-regulated/released during cell stress and injury, acting as a damage-associated molecular pattern molecule (DAMP) that promotes inflammatory processes [24,25]. TLR4 (pattern recognition receptor [PRR] that initiates inflammatory responses), TNFα (cytotoxic and inflammatory cytokine), and ICAM-1 (adhesion molecule that mediates leukocyte adhesion) increased with Chol and EtOH feeding (Fig 3). Increases in these inflammatory molecules were larger after EtOH than Chol. However, EtOH+Chol feeding increased HMGB-1, TLR4, TNFα, and ICAM-1 to an even greater extent than Chol or EtOH alone (Fig 3).

Histologically, leukocyte infiltration increased slightly after Chol and moderately after EtOH. However, leukocyte infiltration was even greater after EtOH+Chol (Fig 1A). MPO (marker of neutrophil infiltration), F4/80 (marker of monocytes/macrophages) and CD4 (marker of T lymphocytes) all increased after Chol and EtOH diets (Fig 4). EtOH caused more leukocyte infiltration than Chol. However, MPO, F4/80 and CD4 all increased to even greater levels in mice fed the EtOH+Chol diet (Fig 4).

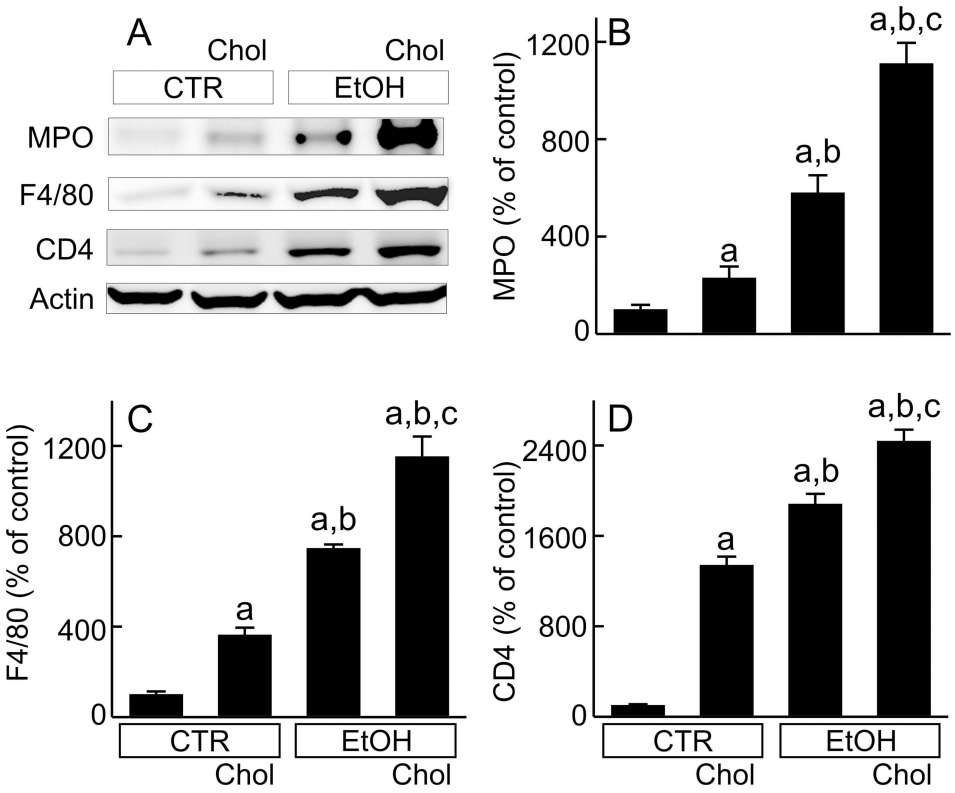

Fig 4. Combined ethanol and cholesterol feeding increases leukocyte infiltration in the liver. Mice were fed CTR, Chol, EtOH and EtOH+Chol diets for 3 months. **A**, representative immunoblots of MPO, F4/80, CD4 and actin. **B**, quantification of MPO immunoblots by densitometry. **C**, quantification of F4/80 immunoblots. **D**, quantification of CD4 immunoblots. Values are means ± S.E.M. **a**, $p < 0.05$ vs CTR; **b**, $p < 0.05$ vs Chol; **c**, $p < 0.05$ vs EtOH (n = 4 per group).

doi:10.1371/journal.pone.0163342.g004

Combined chronic ethanol and cholesterol consumption causes liver fibrosis

After Trichrome staining of liver sections from mice fed CTR and Chol diets, no fibrosis was detected (Fig 5A and 5B). Weak blue Trichrome staining appeared occasionally in some livers of mice fed EtOH (Fig 5C). However after EtOH+Chol, blue Trichrome staining increased in all livers. Fibrosis was predominantly sinusoidal and perivenular (Fig 5D), showing a "chicken-wire" pattern. Bridging fibrosis was present occasionally in some livers of EtOH+Chol-fed mice (Fig 5E).

Fibrosis was further verified by SHG microscopy. In livers of mice fed CTR, collagen SHG signals were barely detectable except around larger vessels (Fig 5F). Collagen SHG signals were unchanged in livers of Chol-fed mice compared to CTR mice (Fig 5G) but increased slightly in some liver from EtOH-fed mice (Fig 5H). By contrast, collagen SHG signals increased markedly in the livers from EtOH+Chol-fed mice. Most of collagen was located along sinusoids and in pericentral regions (Fig 5I), but bridging fibrosis was apparent in some mice (Fig 5J).

By Western blotting, Type I collagen, one of the collagens that form fibers in liver fibrosis, increased 5 folds in Chol-fed mice compared to CTR. In EtOH-fed mice, Type I collagen increased 10 folds. In EtOH+Chol-fed mice, Type I collagen increased to an even greater extent (19 folds) (Fig 5K and 5L).

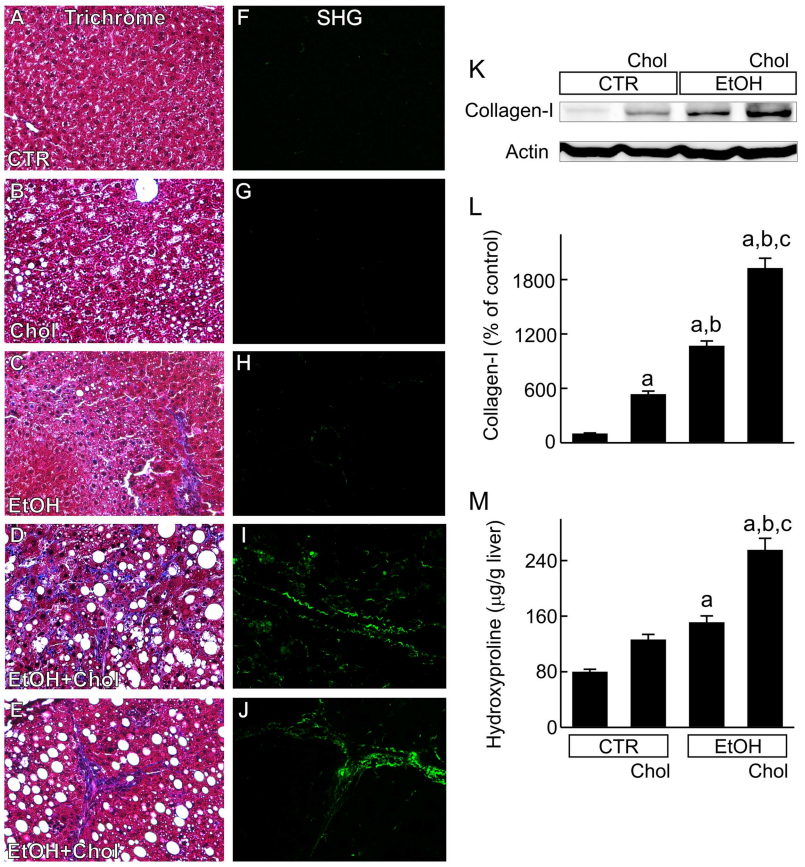

Fig 5. Combined ethanol and cholesterol feeding induces liver fibrosis and increases Type I collagen and hydroxyproline in the liver. Mice were fed CTR, Chol, EtOH and EtOH+Chol diets for 3 months. **A-E**, Mason's Trichrome staining. **F-J**, second harmonic generation (SHG) microscopy. **K**, representative immunoblots of Type I collagen (Collagen-I) and actin. **L**, quantification of Type I collagen immunoblots by densitometry. **M**, hydroxyproline in the liver. Values are means ± S.E.M. **a**, $p < 0.05$ vs CTR; **b**, $p < 0.05$ vs Chol; **c**, $p < 0.05$ vs EtOH ($n = 4$ per group).

doi:10.1371/journal.pone.0163342.g005

Hepatic hydroxyproline, an indicator of collagen deposition, did not increase after Chol feeding but increased modestly after EtOH (Fig 5M). In mice fed EtOH+Chol, hydroxyproline increased more than after Chol and EtOH feeding (Fig 5M).

Combined ethanol plus high cholesterol diet increases hepatic stellate cell activation and alters TGF-β signaling

Activated hepatic stellate cells (HSC) synthesize and excrete extracellular matrix (ECM), leading to liver fibrosis. Expression of α-SMA, a marker of HSC activation, was barely detectable in livers from mice fed CTR (Fig 6A). Hepatic α-SMA increased 3.5 folds in Chol-fed mice and 7.5 folds in EtOH-fed mice. After EtOH+Chol feeding, α-SMA increased to a greater extent than Chol alone or EtOH (11.2 folds) (Fig 6A and 6B).

TGF-β1 is a potent fibrogenic cytokine. TGF-β1 increased 25-fold by Chol feeding, 33-fold by EtOH feeding, and 47-fold by EtOH+Chol feeding (Fig 6A and 6C). BAMBI is a transmembrane TGF-β pseudoreceptor that silences TGF-β signaling [26,27]. BAMBI increased 60% in Chol-fed mice, remained unchanged in EtOH-fed mice, and decreased 30% in EtOH+Chol fed mice (Fig 6A and 6D). miR33a enhances TGF-β profibrogenic effects, possibly by modulating

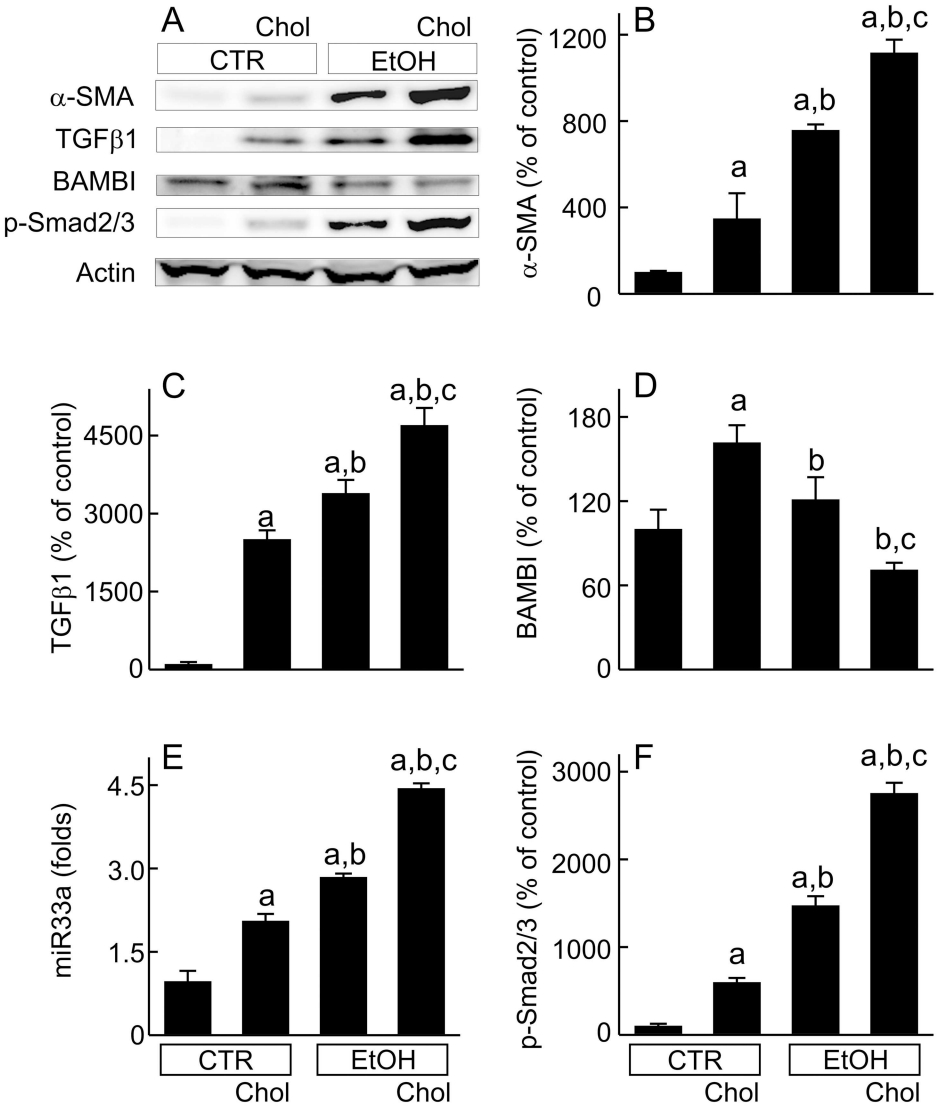

Fig 6. Combined ethanol and cholesterol feeding stimulates stellate cell activation and alters TGF-β signaling in the liver. Mice were fed CTR, Chol, EtOH and EtOH+Chol diets for 3 months. **A**, representative immunoblots of α-SMA, TGF-β1, BAMBI, Smad2/3, phospho-Smad2/3 and actin. **B**, quantification of α-SMA immunoblots by densitometry. **C**, quantification of TGF-β1 immunoblots. **D**, quantification of BAMBI immunoblots. **E**, detection of miR33a by RT-qPCR. **F**, quantification of phospho-Smad2/3 immunoblots. Values are means ± S.E.M. **a**, $p < 0.05$ vs CTR; **b**, $p < 0.05$ vs Chol; **c**, $p < 0.05$ vs EtOH (n = 4 per group).

doi:10.1371/journal.pone.0163342.g006

Smad signaling [28]. miR33a increased 2.0-, 2.8-, and 4.5-fold by Chol, EtOH, and EtOH+Chol feeding, respectively (Fig 6E). Smad2/3 expression was not altered in any groups (not shown). However, phospho-Smad2/3 increased 6-, 15-, and 28-fold by Chol, EtOH and EtOH+Chol feeding, respectively, indicating Smad2/3 activation (Fig 6A and 6F).

Combined ethanol and cholesterol consumption decreases metalloproteinases

MMP degrade ECM. MMP-2 increased slightly (14%) by Chol feeding, was unchanged by EtOH, and decreased 42% by EtOH+Chol (Fig 7A and 7B). MMP-9 was not changed by Chol or EtOH feeding but decreased 44% by EtOH+Chol (Fig 7A and 7C).

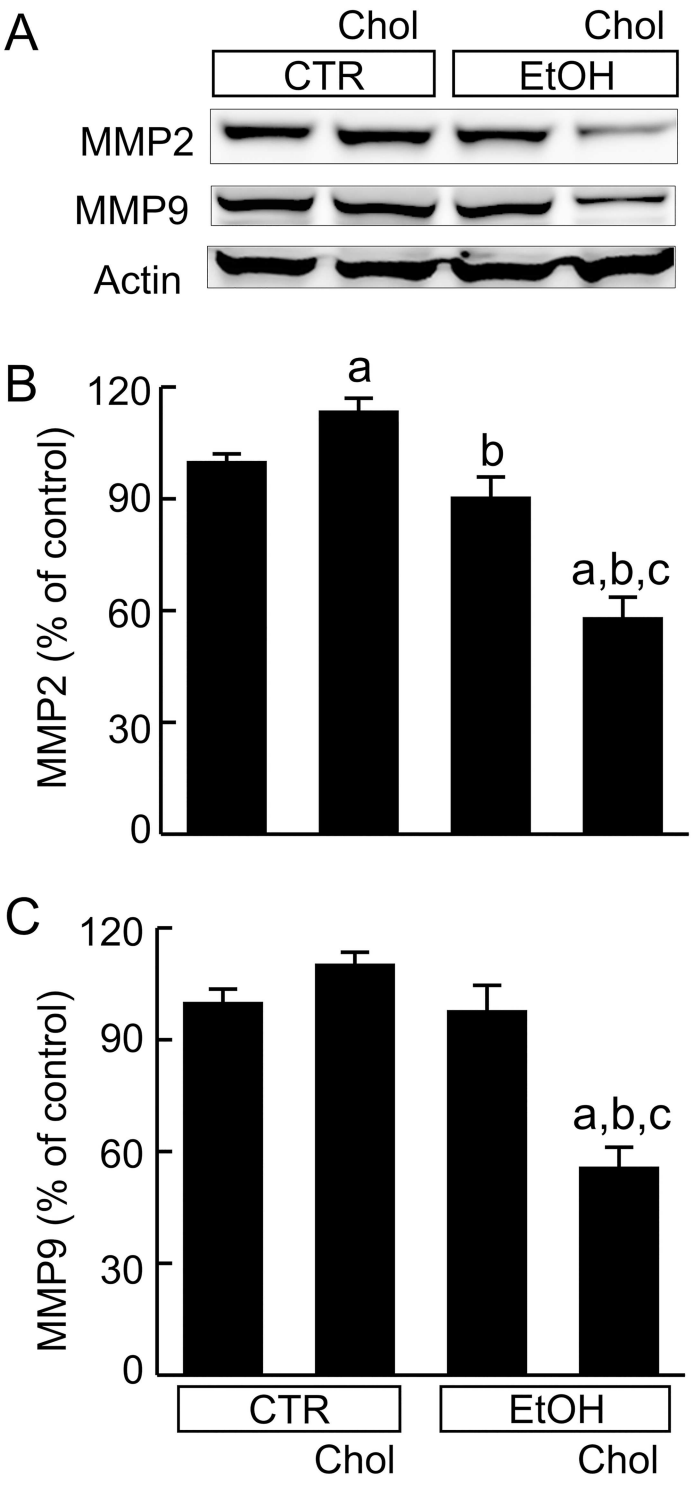

Fig 7. Combined ethanol and cholesterol feeding decreases metalloproteinase expression in the liver. Mice were fed CTR, Chol, EtOH and EtOH+Chol diets for 3 months. **A**, representative immunoblots of MMP-2, MMP-9 and actin. **B**, quantification of MMP-2 immunoblots by densitometry. **C**, quantification of MMP-9 immunoblots. Values are means ± S.E.M. **a**, $p < 0.05$ vs CTR; **b**, $p < 0.05$ vs Chol; **c**, $p < 0.05$ vs EtOH ($n = 4$ per group).

doi:10.1371/journal.pone.0163342.g007

Combined ethanol and cholesterol consumption did not alter ethanol metabolic enzymes but increased oxidative and endoplasmic reticulum stresses

Expression of ADH, Cyp2E1, and ALDH2, enzymes responsible for ethanol metabolism, were not different between EtOH+Chol feeding compared to Chol and EtOH (data not shown). Previous studies show that ethanol increases endoplasmic reticulum (ER) and oxidative stresses [29,30]. Expression of XBP-1 is an indicator of ER stress [31,32]. XBP-1 mRNA was increased slightly by Chol, more by EtOH and greatest by EtOH+Chol feeding (Fig 8A). 4-HNE is an indicator of oxidative stress. Multiple weak bands of 4-HNE adducts were detected in mice fed CTR (Fig 8B). 4-HNE adducts increased slightly after Chol, more after EtOH and greatest after EtOH+Chol (Fig 8B).

Discussion

Combined ethanol and high cholesterol consumption causes severe steatohepatitis and early fibrosis in mice

The pathogenesis of ALD is generally accepted to be a "multi-hit" process involving several risk factors [2,10,33]. In particular, nutritional factors appear to significantly modulate the pathogenesis and progression of alcohol-induced liver injury and fibrosis/cirrhosis [10,11]. Previous studies show that many patients with alcoholic hepatitis have some degree of malnutrition (low calorie and protein intake) [34,35]. High unsaturated fat and fish oil, high fructose intake, iron overload, and zinc deficiency are also reported to increase alcoholic liver injury [13,36–38]. Other studies suggest that high fat diets alter the intestinal microbiome and increase gut permeability, thus increasing endotoxemia and ALD development [37,39]. Obesity also increases the risk of ALD. Overall, nutritional factors and life styles most likely contribute to development of ALD by contributing to one or more of the "multi-hits" in ALD pathogenesis.

Western diets are high in fat and cholesterol. Therefore, excess ethanol consumption often occurs in combination with a high fat and high cholesterol diet. Recent studies show that high dietary cholesterol increases hepatic steatosis, inflammation, fibrosis and cancer in mice, but a high intake and long exposure time (1.5–5% for 25–55 weeks) are required [17,40–42]. Since non-alcoholic steatohepatitis (NASH) and alcoholic steatohepatitis (ASH) have similar pathological changes, we explored the combined effects of chronic ethanol consumption and high cholesterol intake. We showed that chronic cholesterol (0.5% for 12 weeks) alone caused steatosis, mild inflammation and cell death, whereas chronic ethanol alone induced slightly less steatosis than cholesterol but greater inflammation and cell death. Neither EtOH nor Chol diets alone caused observable liver fibrosis (Figs 1–5). By contrast after EtOH+Chol feeding, steatosis, inflammation and cell death all increased markedly over EtOH and Chol, and obvious liver fibrosis occurred (Figs 1–5). These data provide clear evidence that chronic ethanol and high cholesterol synergistically increase ALD development and severity.

Mechanisms by which combined ethanol and high cholesterol consumption exacerbates steatohepatitis

How ethanol and cholesterol synergistically increase steatosis, cell death and inflammation, the three major components of steatohepatitis, remains unclear. Cholesterol does not appear to alter ethanol metabolism, since ADH, Cyp2E1 and ALDH2 expressions were not different in EtOH, Chol and EtOH+Chol groups (data not shown). Increased steatosis could result from increased *de novo* fatty acid synthesis, suppressed fatty acid degradation, and/or inhibited export of lipoproteins from the liver. *De novo* fatty acid synthesis is catalyzed by FAS. However,

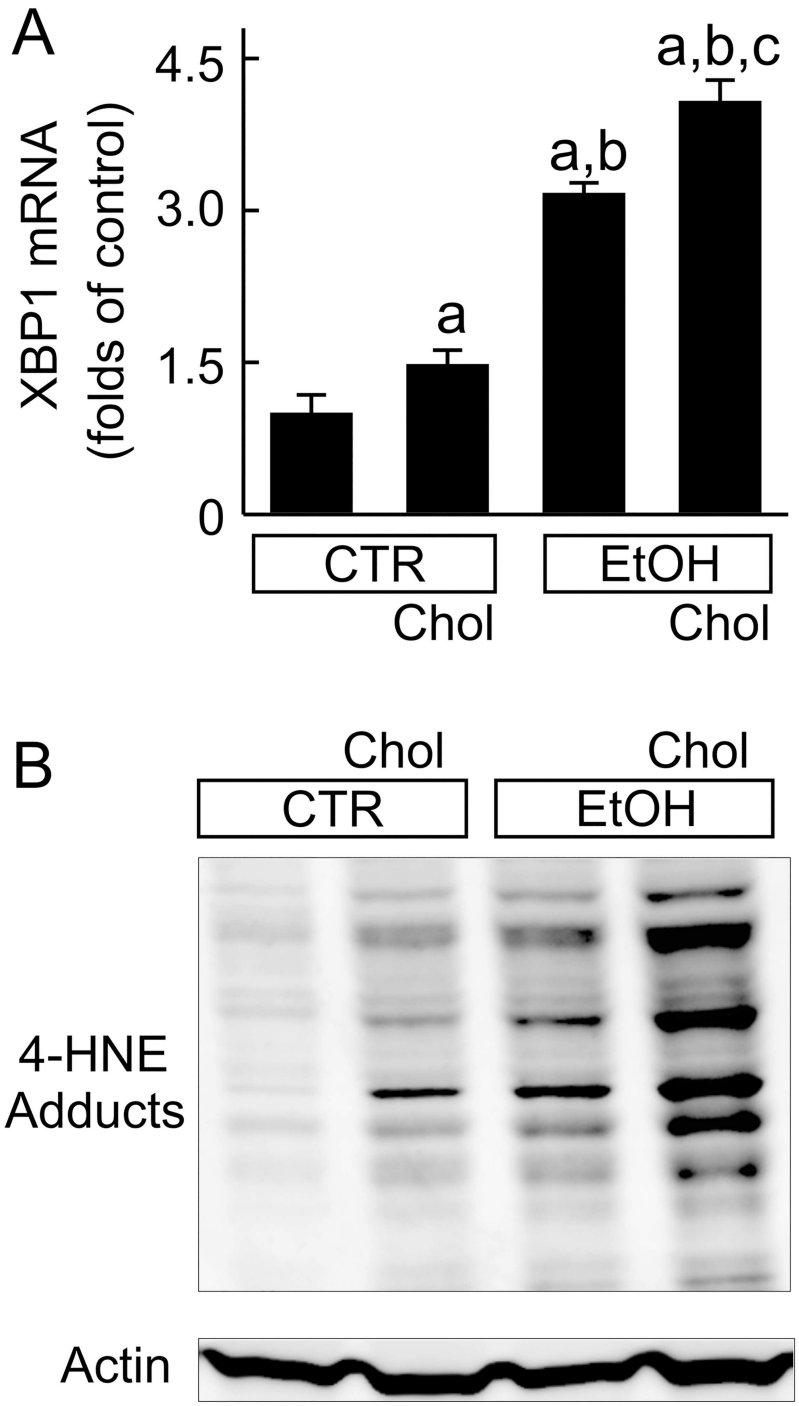

Fig 8. Combined ethanol and cholesterol feeding increases high mobility group box-1 mRNA and 4-hydroxynonenal adduct formation in the liver. Mice were fed CTR, Chol, EtOH and EtOH+Chol diets for 3 months. **A**, XBP-1 mRNA detected by RT-qPCR. Values are means ± S.E.M. **a**, $p < 0.05$ vs CTR; **b**, $p < 0.05$ vs Chol; **c**, $p < 0.05$ vs EtOH ($n = 4$ per group). **B**, representative immunoblots of 4-HNE adducts and actin ($n = 4$ per group).

doi:10.1371/journal.pone.0163342.g008

FAS expression decreased after EtOH+Chol feeding (Fig 2), indicating that hepatic steatosis was not due to increased *de novo* fatty acid synthesis. Alternatively, steatosis may be linked to suppressed fatty acid degradation in mitochondria. Entry of fatty acyl-CoA into mitochondria for β-oxidation is the rate limiting step in fatty acid degradation [23], Cpt1, an enzyme catalyzing an essential step in the transport of long chain fatty acyl-CoA into mitochondria, decreased markedly in EtOH+Chol mice (Fig 2). When mitochondrial uptake and oxidation of fatty acids is inhibited, fatty acyl-CoA is converted to triglyceride. This is consistent with our observed increase in hepatic triglycerides after EtOH+Chol feeding (Fig 2). Such inhibited fatty acid degradation most likely contributes to exacerbated steatosis by EtOH+Chol. Additionally, previous studies show that high dietary cholesterol and alcohol each impair very low density lipoprotein (VLDL) assembly and secretion [43–45]. Therefore, the combination of ethanol and high cholesterol consumption may also inhibit VLDL export, thus exacerbating accumulation of lipids in the liver.

Increased cell death by EtOH+Chol is possibly linked to higher ER and oxidative stresses. Previous studies show that ethanol increases ER stress and stimulates cholesterol trafficking and accumulation into mitochondria, which sensitizes mitochondria to oxidative stress [46]. Other studies also show that ethanol alone increases oxidative stress [47–50]. High cholesterol intake may further exacerbate these pathogenic processes. Indeed, we observed increases in XBP-1 mRNA and 4-HNE adducts in the liver after EtOH+Chol feeding (Fig 8A and 8B), consistent with increased ER and oxidative stresses by combined chronic ethanol and high cholesterol feeding. Oxidative stress is well known to damage macromolecules and organelles (*e.g.*, DNA, proteins, cell membranes, mitochondria). Oxidative damage of membrane lipid components and proteins could compromise ion channels/transporters, enzymes and other plasma membrane activities. Mitochondria, the key bioenergetic organelle, are major producers as well as important targets of ROS [51,52]. Oxidative damage of cardiolipin, a mitochondrial phospholipid that is particularly rich in unsaturated fatty acids [53], suppresses the activity of cytochrome *c* oxidase of the electron transport chain [54]. Oxidative stress also causes onset of the mitochondrial permeability transition [55]. Failure of oxidative phosphorylation decreases ATP production, leading to necrotic cell death. Moreover, mitochondrial release of cytochrome *c* triggers apoptosis [55]. ER stress is also reported to cause apoptosis through mitochondria-dependent and -independent pathways [56]. Thus, combined ethanol and high cholesterol feeding increases cell death, likely by enhancing ER and oxidative stresses.

Increased ER and ROS stresses are also well-known contributors to inflammatory diseases. Activation of serine/threonine-protein kinase/endoribonuclease inositol-requiring enzyme 1 (IRE1) during ER stress recruits TNF receptor associated factor-2 (TRAF2) to the ER membrane to initiate inflammatory responses [57]. PRR activation is also reported to mediate ER stress-induced inflammation [57]. ROS stimulate formation of proinflammary cytokines/chemokines (*e.g.*, TNFα, interleukin-1, CXC chemokine-10) and adhesion molecules [58,59]. Moreover, damage of hepatocytes after ROS and ER stress causes release of proinflammatory damage-associated molecular pattern molecules (DAMPs, *e.g.*, mitochondrial DNA, HMGB1) [60,61]. These potent inflammatory mediators lead to infiltration of leukocytes, which produce more ROS, reactive nitrogen species, and proteases, further amplifying tissue damage.

Whether cholesterol increases inflammation remains controversial. Inflammation is an important component in ALD. Accumulation of free cholesterol in macrophages is a potent inducer of proinflammatory cytokine production [62]. In the liver, high dietary intake of cholesterol upregulates/activates proinflammatory signaling (e.g., NF-κB and TLR4) and increases inflammation in the liver [40,42,63]. High dietary cholesterol also increases production of mitochondrial ROS, which in turn activates the NLRP3 inflammasome [64]. In this study after EtOH+Chol feeding, HMGB-1 (a DAMP), TLR4 (a PRR), TNFα (a cytotoxic and

inflammatory cytokine), and ICAM-1 (an adhesion molecule), all increased markedly in the liver, which was associated with overtly increased infiltration of leukocytes (Figs 1, 3 and 4). Our results support that cholesterol enhances inflammatory signaling after ethanol treatment, possibly by increasing ER and ROS stresses. However, a previous study shows that cholesterol suppresses inflammation in rat livers after ethanol exposure for a month [65]. The reason for this difference remains unclear, perhaps due to differences in species (mice vs rats) and/or duration of treatment. The effects of dietary cholesterol on low-density lipoprotein receptor and cholesterol synthesis are species-dependent, which could result in different cholesterol homeostasis and therefore affect inflammatory responses [66]. Moreover, the previous experiment was shorter (1 month) in duration in comparison to the current study (3 months). Thus, stimulation of the inflammatory response to ethanol by cholesterol may require a longer exposure time.

Mechanisms by which combined ethanol and high cholesterol consumption causes liver fibrosis

Clinically ALD eventually progresses to cirrhosis, culminating liver failure and hepatic carcinoma [3–7]. However, induction of overt liver fibrosis by ethanol feeding in rodents has been difficult, which is an important barrier for development of antifibrotic therapies for ALD. A major difference between human and rodent diets is that normal rodent diets have minimal cholesterol, whereas human diets (especially in the Western countries) have high cholesterol content. It is possible that low cholesterol in rodent diets is the reason for the difficulty of inducing alcoholic fibrosis in rodents. Our study shows that chronic ethanol intake in combination with high cholesterol feeding leads to clearly apparent liver fibrosis with a pathological pattern consistent with alcoholic fibrosis (Fig 5). Thus, chronic ethanol plus high cholesterol feeding represents a new model for studying mechanisms and therapy for alcoholic fibrosis.

A previous study indicates that free cholesterol accumulates in cultured HSC, increasing TLR4 expression and sensitizing HSC to TGF-β [16]. These findings suggest that cholesterol may help to activate HSC *in vitro* and therefore stimulate fibrosis *in vivo*. Indeed, other recent studies show that cholesterol increases fibrosis in NASH in rodents, although this effect requires higher cholesterol (1.5–5%) feeding than used here and for longer periods of time (25–55 weeks) [16,17]. Previous studies also report that acetaldehyde, the reactive metabolite of ethanol, activates HSC in culture [67,68]. In the present study, we found that 0.5% cholesterol feeding alone only slightly increased Type 1 collagen, TGF-β1, α-SMA, and p-Smad 2/3 and did not result in frank fibrosis (Fig 5). BAMBI, a transmembrane TGF-β pseudoreceptor that silences TGF-β signaling [26], increased 60% in cholesterol-fed mice, which may have suppressed fibrosis (Fig 6). Furthermore, MMP2, which degrades ECM, was also slightly increased by cholesterol alone (Fig 7) to further delay fibrosis.

EtOH feeding alone caused somewhat greater pro-fibrotic responses compared to Chol alone (Figs 6 and 7), but outright fibrosis was still minimal (Fig 5). Although Chol and EtOH individually did not cause visible fibrosis, combined EtOH+Chol feeding caused definitive liver fibrosis (Fig 5). HSC activation, collagen formation and deposition, TGF-β and downstream TGF-β signaling all increased to much higher levels after EtOH+Chol feeding than after Chol or EtOH alone. Moreover, BAMBI and MMPs decreased 30–44% by EtOH+Chol (Figs 5–7). Together, these data indicated substantially increased profibrotic responses with decreased antifibrotic responses after EtOH+Chol feeding. Increased TGF-β is possibly linked to higher oxidative stress after EtOH+Chol feeding, since synthesis and activation of TGF-β, the key fibrogenetic cytokine, are stimulated by oxidative stress [69]. ER stress is also reported to induce fibrogenic responses in hepatic stellate cells [70]. Cholesterol homeostasis is regulated

by sterol regulatory element-binding protein-2 (SREBP2) [16]. A recent study shows that high fat plus high cholesterol diet increases hepatic SREBP2 [16]. ER stress also stimulates expression of SREBPs [71]. Interestingly, the primary transcript of SREBP2 encodes miR33a, a micro RNA that enhances TGF-β/Smad signaling [16]. Therefore, increased SREBP2 may also increase miR33a formation and thus augment fibrosis. Indeed, miR33a markedly increased after EtOH+Chol feeding (Fig 6).

Taken together, this study demonstrated that combined ethanol and cholesterol consumption synergistically increased liver steatosis, injury, inflammation and fibrosis. These effects were most likely linked to oxidative and ER stresses, increased proinflammatory and profibrotic cytokine formation, and suppressed antifibrotic responses. Combined ethanol and cholesterol consumption mimics the Western diet style and provides a useful animal model for studying alcoholic steatohepatitis and liver fibrosis.

Acknowledgments

This work was supported, in part, by Grants AA017756, DK073336 and DK037034 from the National Institutes of Health. The Cell & Molecular Imaging Core of the Hollings Cancer Center at the Medical University of South Carolina supported by NIH Grant 1P30 CA138313 and the Shared Instrumentation Grant S10 OD018113 provided instrumentation and assistance for SHG microscopy. Animals were housed in the Animal Resources at Medical University of South Carolina supported by NIH Grant C06 RR015455. The funders had no role in study design, data collection and analysis, decision to publish, or preparation of the manuscript.

Author Contributions

Conceptualization: ZZ.

Data curation: YK ZZ.

Formal analysis: YK ZZ.

Funding acquisition: ZZ JJL.

Investigation: YK VKR MG ZZ.

Methodology: YK VKR ZZ.

Project administration: ZZ.

Resources: ZZ JJL.

Supervision: ZZ.

Validation: ZZ.

Writing – original draft: ZZ YK.

Writing – review & editing: JJL RGS.

References

1. Ishak KG, Zimmerman HJ, Ray MB (1991) Alcoholic liver disease: pathologic, pathogenetic and clinical aspects. Alcohol Clin Exp Res 15: 45–66. PMID: 2059245
2. Bataller R, Gao B (2015) Liver fibrosis in alcoholic liver disease. Semin Liver Dis 35: 146–156. doi: 10.1055/s-0035-1550054 PMID: 25974900
3. Grant BF (1992) Prevalence of the proposed DSM-IV alcohol use disorders: United States, 1988. Br J Addict 87: 309–316. PMID: 1555008

4. Jamal MM, Morgan TR (2003) Liver disease in alcohol and hepatitis C. Best Pract Res Clin Gastroenterol 17: 649–662. PMID: 12828960
5. Mandayam S, Jamal MM, Morgan TR (2004) Epidemiology of alcoholic liver disease. Semin Liver Dis 24: 217–232. PMID: 15349801
6. Voigt MD (2005) Alcohol in hepatocellular cancer. Clin Liver Dis 9: 151–169. S1089-3261(04)00115-1 [pii];doi: 10.1016/j.cld.2004.10.003 PMID: 15763234
7. Gao B, Bataller R (2011) Alcoholic Liver Disease: Pathogenesis and New Therapeutic Targets. Gastroenterology. S0016-5085(11)01228-5 [pii];doi: 10.1053/j.gastro.2011.09.002
8. Felver ME, Mezey E, McGuire M, Mitchell MC, Herlong HF, Veech GA, et al. (1990) Plasma tumor necrosis factor α predicts decreased long term survival in severe alcoholic hepatitis. Alcohol Clin Exp Res 14: 255–259. PMID: 2190492
9. Moreno C, Langlet P, Hittelet A, Lasser L, Degre D, Evrard S, et al. (2010) Enteral nutrition with or without N-acetylcysteine in the treatment of severe acute alcoholic hepatitis: a randomized multicenter controlled trial. J Hepatol 53: 1117–1122. S0168-8278(10)00683-5 [pii];doi: 10.1016/j.jhep.2010.05.030 PMID: 20801542
10. Beier JI, Arteel GE, McClain CJ (2011) Advances in alcoholic liver disease. Curr Gastroenterol Rep 13: 56–64. doi: 10.1007/s11894-010-0157-5 PMID: 21088999
11. Nanji AA, French SW (1986) Dietary factors and alcoholic cirrhosis. Alcohol Clin Exp Res 10: 271–273. PMID: 3526949
12. Mendenhall C, Roselle GA, Gartside P, Moritz T (1995) Relationship of protein calorie malnutrition to alcoholic liver disease: a reexamination of data from two Veterans Administration Cooperative Studies. Alcohol Clin Exp Res 19: 635–641. PMID: 7573786
13. Bosma A, Seifert WF, van Thiel-de Ruiter GC, van Leeuwen RE, Blauw B, Roholl P, et al. (1994) Alcohol in combination with malnutrition causes increased liver fibrosis in rats. J Hepatol 21: 394–402. S0168-8278(05)80319-8 [pii]. PMID: 7836710
14. Nanji AA, Mendenhall CL, French SW (1989) Beef fat prevents alcoholic liver disease in the rat. Alcohol Clin Exp Res 13: 15–19. PMID: 2646971
15. Ioannou GN, Morrow OB, Connole ML, Lee SP (2009) Association between dietary nutrient composition and the incidence of cirrhosis or liver cancer in the United States population. Hepatology 50: 175–184. doi: 10.1002/hep.22941 PMID: 19441103
16. Tomita K, Teratani T, Suzuki T, Shimizu M, Sato H, Narimatsu K, et al. (2014) Free cholesterol accumulation in hepatic stellate cells: mechanism of liver fibrosis aggravation in nonalcoholic steatohepatitis in mice. Hepatology 59: 154–169. doi: 10.1002/hep.26604 PMID: 23832448
17. Teratani T, Tomita K, Suzuki T, Oshikawa T, Yokoyama H, Shimamura K, et al. (2012) A high-cholesterol diet exacerbates liver fibrosis in mice via accumulation of free cholesterol in hepatic stellate cells. Gastroenterology 142: 152–164. S0016-5085(11)01375-8 [pii];doi: 10.1053/j.gastro.2011.09.049 PMID: 21995947
18. Zhong Z, Ramshesh VK, Rehman H, Liu Q, Theruvath TP, Krishnasamy Y, et al. (2014) Acute ethanol causes hepatic mitochondrial depolarization in mice: role of ethanol metabolism. PLoS One 9: e91308. doi: 10.1371/journal.pone.0091308 PONE-D-13-19739 [pii]. PMID: 24618581
19. Reddy GK, Enwemeka CS (1996) A simplified method for the analysis of hydroxyproline in biological tissues. Clin Biochem 29: 225–229. 0009912096000036 [pii]. PMID: 8740508
20. Rehman H, Ramshesh VK, Theruvath TP, Kim I, Currin RT, Giri S, et al. (2008) NIM811, a Mitochondrial Permeability Transition Inhibitor, Attenuates Cholestatic Liver Injury But Not Fibrosis in Mice. J Pharmacol Exp Ther 327: 699–706. doi: 10.1124/jpet.108.143578 PMID: 18801946
21. Campagnola PJ, Loew LM (2003) Second-harmonic imaging microscopy for visualizing biomolecular arrays in cells, tissues and organisms. Nat Biotechnol 21: 1356–1360. doi: 10.1038/nbt894; nbt894 [pii]. PMID: 14595363
22. Rehman H, Liu Q, Krishnasamy Y, Shi Z, Ramshesh VK, Haque K, et al. (2016) The mitochondria-targeted antioxidant MitoQ attenuates liver fibrosis in mice. Int J Physiol Pathophysiol Pharmacol 8: 14–27. PMID: 27186319
23. Bonnefont JP, Djouadi F, Prip-Buus C, Gobin S, Munnich A, Bastin J (2004) Carnitine palmitoyltransferases 1 and 2: biochemical, molecular and medical aspects. Mol Aspects Med 25: 495–520. doi: 10.1016/j.mam.2004.06.004; S0098299704000494 [pii]. PMID: 15363638
24. Zhai Y, Busuttil RW, Kupiec-Weglinski JW (2011) Liver ischemia and reperfusion injury: new insights into mechanisms of innate-adaptive immune-mediated tissue inflammation. Am J Transplant 11: 1563–1569. doi: 10.1111/j.1600-6143.2011.03579.x PMID: 21668640

25. Boros P, Bromberg JS (2006) New cellular and molecular immune pathways in ischemia/reperfusion injury. Am J Transplant 6: 652–658. AJT1228 [pii];doi: 10.1111/j.1600-6143.2005.01228.x PMID: 16539620

26. Onichtchouk D, Chen YG, Dosch R, Gawantka V, Delius H, Massague J, et al. (1999) Silencing of TGF-beta signalling by the pseudoreceptor BAMBI. Nature 401: 480–485. doi: 10.1038/46794 PMID: 10519551

27. Seki E, De M S, Osterreicher CH, Kluwe J, Osawa Y, et al. (2007) TLR4 enhances TGF-beta signaling and hepatic fibrosis. Nat Med 13: 1324–1332. PMID: 17952090

28. Huang CF, Sun CC, Zhao F, Zhang YD, Li DJ (2015) miR-33a levels in hepatic and serum after chronic HBV-induced fibrosis. J Gastroenterol 50: 480–490. doi: 10.1007/s00535-014-0986-3 PMID: 25155445

29. Ji C, Kaplowitz N (2003) Betaine decreases hyperhomocysteinemia, endoplasmic reticulum stress, and liver injury in alcohol-fed mice. Gastroenterology 124: 1488–1499. S0016508503002762 [pii]. PMID: 12730887

30. Galligan JJ, Smathers RL, Shearn CT, Fritz KS, Backos DS, Jiang H, et al. (2012) Oxidative Stress and the ER Stress Response in a Murine Model for Early-Stage Alcoholic Liver Disease. J Toxicol 2012: 207594. doi: 10.1155/2012/207594 PMID: 22829816

31. Lee AH, Iwakoshi NN, Glimcher LH (2003) XBP-1 regulates a subset of endoplasmic reticulum resident chaperone genes in the unfolded protein response. Mol Cell Biol 23: 7448–7459. PMID: 14559994

32. Iwakoshi NN, Lee AH, Vallabhajosyula P, Otipoby KL, Rajewsky K, Glimcher LH (2003) Plasma cell differentiation and the unfolded protein response intersect at the transcription factor XBP-1. Nat Immunol 4: 321–329. doi: 10.1038/ni907; ni907 [pii]. PMID: 12612580

33. Enomoto N, Takei Y, Yamashina S, Ikejima K, Kitamura T, Sato N (2007) Anti-inflammatory strategies in alcoholic steatohepatitis. J Gastroenterol Hepatol 22 Suppl 1: S59–S61. JGH4652 [pii];doi: 10.1111/j.1440-1746.2006.04652.x PMID: 17567468

34. Mendenhall CL, Anderson S, Weesner RE, Goldberg SJ, Crolic KA (1984) Protein-calorie malnutrition associated with alcoholic hepatitis. Veterans Administration Cooperative Study Group on Alcoholic Hepatitis. Am J Med 76: 211–222. PMID: 6421159

35. Mendenhall CL, Moritz TE, Roselle GA, Morgan TR, Nemchausky BA, Tamburro CH, et al. (1995) Protein energy malnutrition in severe alcoholic hepatitis: diagnosis and response to treatment. The VA Cooperative Study Group #275. JPEN J Parenter Enteral Nutr 19: 258–265. PMID: 8523623

36. Mohammad MK, Zhou Z, Cave M, Barve A, McClain CJ (2012) Zinc and liver disease. Nutr Clin Pract 27: 8–20. 27/1/8 [pii];doi: 10.1177/0884533611433534 PMID: 22307488

37. Kirpich IA, Feng W, Wang Y, Liu Y, Beier JI, Arteel GE, et al. (2013) Ethanol and dietary unsaturated fat (corn oil/linoleic acid enriched) cause intestinal inflammation and impaired intestinal barrier defense in mice chronically fed alcohol. Alcohol 47: 257–264. S0741-8329(13)00023-2 [pii];doi: 10.1016/j.alcohol.2013.01.005 PMID: 23453163

38. Dostalikova-Cimburova M, Balusikova K, Kratka K, Chmelikova J, Hejda V, Hnanicek J, et al. (2014) Role of duodenal iron transporters and hepcidin in patients with alcoholic liver disease. J Cell Mol Med 18: 1840–1850. doi: 10.1111/jcmm.12310 PMID: 24894955

39. Vassallo G, Mirijello A, Ferrulli A, Antonelli M, Landolfi R, Gasbarrini A, et al. (2015) Review article: Alcohol and gut microbiota—the possible role of gut microbiota modulation in the treatment of alcoholic liver disease. Aliment Pharmacol Ther 41: 917–927. doi: 10.1111/apt.13164 PMID: 25809237

40. Wouters K, van Gorp PJ, Bieghs V, Gijbels MJ, Duimel H, Lutjohann D, et al. (2008) Dietary cholesterol, rather than liver steatosis, leads to hepatic inflammation in hyperlipidemic mouse models of nonalcoholic steatohepatitis. Hepatology 48: 474–486. doi: 10.1002/hep.22363 PMID: 18666236

41. Sumiyoshi M, Sakanaka M, Kimura Y (2010) Chronic intake of a high-cholesterol diet resulted in hepatic steatosis, focal nodular hyperplasia and fibrosis in non-obese mice. Br J Nutr 103: 378–385. S0007114509991772 [pii];doi: 10.1017/S0007114509991772 PMID: 19818196

42. Kampschulte M, Stockl C, Langheinrich AC, Althohn U, Bohle RM, Krombach GA, et al. (2014) Western diet in ApoE-LDLR double-deficient mouse model of atherosclerosis leads to hepatic steatosis, fibrosis, and tumorigenesis. Lab Invest 94: 1273–1282. labinvest2014112 [pii];doi: 10.1038/labinvest.2014.112 PMID: 25199052

43. Cote I, Chapados NA, Lavoie JM (2014) Impaired VLDL assembly: a novel mechanism contributing to hepatic lipid accumulation following ovariectomy and high-fat/high-cholesterol diets? Br J Nutr 112: 1592–1600. S0007114514002517 [pii];doi: 10.1017/S0007114514002517 PMID: 25263431

44. Savard C, Tartaglione EV, Kuver R, Haigh WG, Farrell GC, Subramanian S, et al. (2013) Synergistic interaction of dietary cholesterol and dietary fat in inducing experimental steatohepatitis. Hepatology 57: 81–92. doi: 10.1002/hep.25789 PMID: 22508243

45. Kharbanda KK, Todero SL, Ward BW, Cannella JJ III, Tuma DJ (2009) Betaine administration corrects ethanol-induced defective VLDL secretion. Mol Cell Biochem 327: 75–78. doi: 10.1007/s11010-009-0044-2 PMID: 19219625

46. Mari M, Morales A, Colell A, Garcia-Ruiz C, Fernandez-Checa JC (2014) Mitochondrial cholesterol accumulation in alcoholic liver disease: Role of ASMase and endoplasmic reticulum stress. Redox Biol 3: 100–108. S2213-2317(14)00104-9 [pii];doi: 10.1016/j.redox.2014.09.005 PMID: 25453982

47. Fromenty B, Grimbert S, Mansouri A, Beaugrand M, Erlinger S, Rotig A, et al. (1995) Hepatic mitochondrial DNA deletion in alcoholics: association with microvesicular steatosis. Gastroenterology 108: 193–200. PMID: 7806041

48. Fromenty B, Pessayre D (1995) Inhibition of mitochondrial beta-oxidation as a mechanism of hepatotoxicity. Pharmacol Ther 67: 101–154. PMID: 7494860

49. Fernandez-Checa JC, Kaplowitz N (2005) Hepatic mitochondrial glutathione: transport and role in disease and toxicity. Toxicol Appl Pharmacol 204: 263–273. PMID: 15845418

50. Matsuhashi T, Karbowski M, Liu X, Usukura J, Wozniak M, Wakabayashi T (1998) Complete suppression of ethanol-induced formation of megamitochondria by 4-hydroxy-2,2,6,6-tetramethyl-piperidine-1-oxyl (4-OH-TEMPO). Free Radic Biol Med 24: 139–147. PMID: 9436623

51. Lemasters JJ, Theruvath TP, Zhong Z, Nieminen AL (2009) Mitochondrial calcium and the permeability transition in cell death. Biochim Biophys Acta 1787: 1395–1401. S0005-2728(09)00222-9 [pii];doi: 10.1016/j.bbabio.2009.06.009 PMID: 19576166

52. Birch-Machin MA, Turnbull DM (2001) Assaying mitochondrial respiratory complex activity in mitochondria isolated from human cells and tissues. Methods Cell Biol 65: 97–117. PMID: 11381612

53. Robinson NC (1993) Functional binding of cardiolipin to cytochrome c oxidase. J Bioenerg Biomembr 25: 153–163. PMID: 8389748

54. Paradies G, Petrosillo G, Pistolese M, Ruggiero FM (2000) The effect of reactive oxygen species generated from the mitochondrial electron transport chain on the cytochrome c oxidase activity and on the cardiolipin content in bovine heart submitochondrial particles. FEBS Lett 466: 323–326. S0014-5793(00)01082-6 [pii]. PMID: 10682852

55. Kim JS, He L, Lemasters JJ (2003) Mitochondrial permeability transition: a common pathway to necrosis and apoptosis. Biochem Biophys Res Commun 304: 463–470. PMID: 12729580

56. Foufelle F, Fromenty B (2016) Role of endoplasmic reticulum stress in drug-induced toxicity. Pharmacol Res Perspect 4: e00211. doi: 10.1002/prp2.211; PRP2211 [pii]. PMID: 26977301

57. Keestra-Gounder AM, Byndloss MX, Seyffert N, Young BM, Chavez-Arroyo A, Tsai AY, et al. (2016) NOD1 and NOD2 signalling links ER stress with inflammation. Nature. nature17631 [pii];doi: 10.1038/nature17631

58. Jaeschke H, Ho YS, Fisher MA, Lawson JA, Farhood A (1999) Glutathione peroxidase-deficient mice are more susceptible to neutrophil-mediated hepatic parenchymal cell injury during endotoxemia: importance of an intracellular oxidant stress. Hepatology 29: 443–450. S027091399900066X [pii];doi: 10.1002/hep.510290222 PMID: 9918921

59. Czaja MJ (2007) Cell signaling in oxidative stress-induced liver injury. Semin Liver Dis 27: 378–389. doi: 10.1055/s-2007-991514 PMID: 17979074

60. Chen R, Hou W, Zhang Q, Kang R, Fan XG, Tang D (2013) Emerging role of high-mobility group box 1 (HMGB1) in liver diseases. Mol Med 19: 357–366. molmed.2013.00099 [pii];doi: 10.2119/molmed.2013.00099

61. Gauley J, Pisetsky DS (2009) The translocation of HMGB1 during cell activation and cell death. Autoimmunity 42: 299–301. doi: 10.1080/08916930902831522 [pii]. PMID: 19811282

62. Li Y, Schwabe RF, DeVries-Seimon T, Yao PM, Gerbod-Giannone MC, Tall AR, et al. (2005) Free cholesterol-loaded macrophages are an abundant source of tumor necrosis factor-alpha and interleukin-6: model of NF-kappaB- and map kinase-dependent inflammation in advanced atherosclerosis. J Biol Chem 280: 21763–21772. M501759200 [pii];doi: 10.1074/jbc.M501759200 PMID: 15826936

63. Strekalova T, Costa-Nunes JP, Veniaminova E, Kubatiev A, Lesch KP, Chekhonin VP, et al. (2016) Insulin receptor sensitizer, dicholine succinate, prevents both Toll-like receptor 4 (TLR4) upregulation and affective changes induced by a high-cholesterol diet in mice. J Affect Disord 196: 109–116. S0165-0327(15)30949-6 [pii];doi: 10.1016/j.jad.2016.02.045 PMID: 26921863

64. Du Q, Wang Q, Fan H, Wang J, Liu X, Wang H, et al. (2016) Dietary cholesterol promotes AOM-induced colorectal cancer through activating the NLRP3 inflammasome. Biochem Pharmacol. S0006-2952(16)00116-7 [pii];doi: 10.1016/j.bcp.2016.02.017

65. Nanji AA, Rahemtulla A, Daly T, Khwaja S, Miao L, Zhao S, et al. (1997) Cholesterol supplementation prevents necrosis and inflammation but enhances fibrosis in alcoholic liver disease in the rat. Hepatology 26: 90–97. PMID: 9214456

66. Roach PD, Balasubramaniam S, Hirata F, Abbey M, Szanto A, Simons LA, et al. (1993) The low-density lipoprotein receptor and cholesterol synthesis are affected differently by dietary cholesterol in the rat. Biochim Biophys Acta 1170: 165–172. 0005-2760(93)90067-J [pii]. PMID: 8399341

67. Wang H, Guan W, Yang W, Wang Q, Zhao H, Yang F, et al. (2014) Caffeine inhibits the activation of hepatic stellate cells induced by acetaldehyde via adenosine A2A receptor mediated by the cAMP/PKA/SRC/ERK1/2/P38 MAPK signal pathway. PLoS One 9: e92482. doi: 10.1371/journal.pone.0092482; PONE-D-13-53472 [pii]. PMID: 24682220

68. Reyes-Gordillo K, Shah R, Arellanes-Robledo J, Hernandez-Nazara Z, Rincon-Sanchez AR, Inagaki Y, et al. (2014) Mechanisms of action of acetaldehyde in the up-regulation of the human alpha2(I) collagen gene in hepatic stellate cells: key roles of Ski, SMAD3, SMAD4, and SMAD7. Am J Pathol 184: 1458–1467. S0002-9440(14)00094-7 [pii];doi: 10.1016/j.ajpath.2014.01.020 PMID: 24641900

69. Sanchez-Valle V, Chavez-Tapia NC, Uribe M, Mendez-Sanchez N (2012) Role of oxidative stress and molecular changes in liver fibrosis: a review. Curr Med Chem 19: 4850–4860. CMC-EPUB-20120618-9 [pii]. PMID: 22709007

70. Hernandez-Gea V, Hilscher M, Rozenfeld R, Lim MP, Nieto N, Werner S, et al. (2013) Endoplasmic reticulum stress induces fibrogenic activity in hepatic stellate cells through autophagy. J Hepatol 59: 98–104. S0168-8278(13)00138-4 [pii];doi: 10.1016/j.jhep.2013.02.016 PMID: 23485523

71. Werstuck GH, Lentz SR, Dayal S, Hossain GS, Sood SK, Shi YY, et al. (2001) Homocysteine-induced endoplasmic reticulum stress causes dysregulation of the cholesterol and triglyceride biosynthetic pathways. J Clin Invest 107: 1263–1273. doi: 10.1172/JCI11596 PMID: 11375416